

Different right ventricular contractility in limited cutaneous systemic sclerosis-associated pulmonary arterial hypertension and idiopathic pulmonary arterial hypertension

Maria J. Overbeek ^{*}, Jan-Willem Lankhaar ^{*†}, Nico Westerhof ^{*‡}, Alexandre E. Voskuyl [§], Anco Boonstra, ^{*}, Jean G.F. Bronzwaer ^{||}, Koen M.J. Marques ^{||}, Egbert F. Smit ^{*}, Ben A C. Dijkmans [§], Anton Vonk Noordegraaf ^{*}

Departments of ^{*}Pulmonary Diseases, [†]Physics and Medical Technology, [‡]Physiology, [§]Rheumatology, ^{||}Cardiology

Institute for Cardiovascular Research. VU University Medical Center, Amsterdam

Name and Address for Correspondence:

Dr. Anton Vonk Noordegraaf
Department of Pulmonary Diseases
VU University Medical Center
De Boelelaan 1117
P.O. Box 7057
1007 MB Amsterdam, The Netherlands
e-mail: A.Vonk@VUmc.nl
tel: +31-20-4441886
fax: +31-20-4444328

Funding: Netherlands Heart Foundation (NHS2003B274 to J.W.L).

Short title: Right ventricular contractility in SScPAH

Abstract

Since systemic sclerosis (SSc) also involves the heart, we evaluated possible differences in right ventricular (RV) pump function between SSc-associated pulmonary arterial hypertension (SScPAH) and idiopathic PAH (IPAH).

In 13 limited cutaneous SScPAH and 17 IPAH-patients, RV pump function was described by the pump function graph, which relates mean RV pressure (mPrv) and stroke volume index (SVI). Differences in pump function result in shift or rotation of the pump function graph. Mean Prv and SVI were measured by standard catheterization. The mean of the hypothetical RV isovolumic pressure (mPrv_{iso}) was estimated using a single-beat method. The pump function graph was approximated by a parabola: $mPrv = mPrv_{iso} [1 - (SVI/SVI_{max})^2]$, enabling calculation of SVI_{max}, the hypothetical maximal SVI at zero mPrv.

There were no differences in SVI and SVI_{max}. Both mPrv and mPrv_{iso} were significantly lower in SScPAH than in IPAH (mPrv: 30.7 ± 8.5 vs. 41.2 ± 9.4 mmHg, $p = 0.006$; mPrv_{iso}: 43.1 ± 12.4 vs. 53.5 ± 10.0 mmHg, $p = 0.04$). Since higher pressures were found at similar SVI, the difference in pump function graph results from a lower contractility in SScPAH than in IPAH.

RV contractility is lower in SScPAH than in IPAH.

Key words: myocardial contraction, pump function graph, right ventricular function, right ventricular pressure, stroke volume

Introduction

Patients with systemic sclerosis (SSc) are at high risk of developing pulmonary arterial hypertension (PAH) with estimated prevalences between 7.9 and 12 % (1, 2). SScPAH has a higher risk of death than patients with idiopathic PAH (IPAH), as demonstrated by Kawut *et al.* and Fisher *et al.* (3, 4). These differences have not been explained satisfactorily so far, but co-morbidity due to the systemic character of SSc, age-related factors due to the later disease onset of PAH in SSc and differences in pulmonary vasculopathy (5) may all play a role. In addition, the SScPAH patients described by Kawut and Fisher had a higher mortality despite a similar or lower pulmonary vascular resistance (PVR) at baseline (3, 4). This suggests an inferior ability of the SScPAH right ventricle to adapt to the arterial load compared to the IPAH right ventricle. We therefore hypothesize that right ventricular contractility is impaired in SScPAH when compared to IPAH.

To test this hypothesis, we first characterized possible differences in cardiac output, right ventricular pressure and arterial load in terms of pulmonary vascular resistance (PVR) and pulmonary arterial compliance (C) between the two groups. Then we characterized right ventricular pump function in both groups using the pump function graph (6), describing the cardiac pumping ability by the relationship between mean right ventricular pressure (mPrv) and cardiac output.

Material and Methods

Study design

We included patients diagnosed with SScPAH (n=13) or IPAH (n=17) at the VU University medical center between July 2000 and July 2006 and of whom PRV and pulmonary artery pressure (PAP) waveforms were recorded and digitally stored during standard right heart catheterisation. The study was approved by the Institutional Review Board on Research Involving Human Subjects of the VU University Medical Center

Methods

Pulmonary hypertension was confirmed by a mean PAP (mPap) of > 25 mmHg at rest measured, a pulmonary capillary wedge pressure (PCWP) of < 15 mmHg. All catheterisations were baseline measurements. Additional clinical diagnostic work up was performed according to a standard diagnostic protocol (7) to exclude other causes of pulmonary hypertension. The diagnosis of systemic sclerosis was based on the classification criteria proposed by LeRoy *et al.*(8)

Pulmonary function testing (\dot{V}_{\max} 229 and 6200; SensorMedics; Yorba Linda, CA) and high resolution computed tomography (HRCT; CT Somatom Plus 4; Siemens; Erlangen; Germany) were used to exclude underlying fibrotic lung disease as a cause of pulmonary hypertension.

Analysis

Haemodynamic parameters

Cardiac output (CO) was calculated by the Fick method and PVR was calculated by $(\text{mPap} - \text{PCWP})/\text{CO}$. The RV pressure waveform was averaged to obtain mPrv. Stroke volume index (SVI) was calculated as cardiac index (CI) divided by heart rate (HR). Total pulmonary arterial compliance was calculated as stroke volume (SV) divided by pulse pressure (PP)(9,

10). PP was calculated as systolic PAP minus diastolic PAP. Pressure measurements were recorded digitally at a sampling frequency of 250 Hz using a customized LabView data-acquisition system (National Instruments Netherlands B.V., Woerden, the Netherlands).

Pump Function Graph

For the characterization of RV pump function, we constructed a pump function graph. The pump function graph describes pump function quantitatively by the relationship between mPrv and cardiac output. Experimentally, this relationship has been determined by making the heart beat against a series of different arterial loads. Here we use stroke volume index (SVI) instead of cardiac output to avoid possible confounding effects of differences in heart rate and to normalize for body size. A pump function graph with the effects of alterations in diastolic filling and contractility is shown schematically in Figure 1.

From the digitally recorded RV pressure waveform and SVI, we were able to obtain individual pump function graphs as follows. The pump function graph was approximated by a parabola (11):

$$mPrv = mPrv_{iso} [1 - (SVI/SVI_{max})^2]$$

with mPrv the (time)average of the RV pressure waveform, mPrv_{iso} the average of the RV pressure waveform of an isovolumic beat and SVI_{max} the intercept with the SVI axis, i.e., the hypothetical maximal SVI at zero mPrv. The mPrv and SVI were measured at catheterisation and give the working point (Figure 1).

Subsequently, an estimate of the isovolumic RV pressure waveform, Prv_{iso} was obtained by the single-beat method originally proposed by Sunagawa *et al.*(12) and validated for the RV by Brimiouille *et al.*(13). Its average value is mPrv_{iso}, and since for an isovolumic beat SVI is zero by definition, this yielded the second point of the pump function graph. Finally, SVI_{max} was obtained by rewriting the above equation as:

$$SVI_{\max} = SVI / \sqrt{1 - mPrv / mPrv_{\text{iso}}}$$

and inserting the measured values of SVI and mPrv, and the calculated value of mPrv_{iso}. Since SVI_{max} represents the intercept at the SVI-axis, this yielded the third point of the graph. The three points are indicated in Figure 1.

The single-beat method assumes that the pressure waveform of an isovolumic beat can be described by a sinusoidal function and that it can be obtained by a least-squares fit to the isovolumic phases of the RV pressure waveform of the ejecting beat. Isovolumic contraction was assumed to start at the minimum RV pressure before the steep rise of the pressure (R-wave of ECG), and to end when Prv reached diastolic pulmonary artery pressure. The isovolumic relaxation period was defined from pulmonary artery valve closure, identified by overlaying the pulmonary artery pressure waveform over the RV pressure waveform, till the ventricular pressure reached the diastolic pressure level from which the isovolumic contraction calculations were started. A schematic example is shown in Figure 2. Before the analysis, underdamping catheter artifacts were removed from the pressure waveforms with a Butterworth filter (cut-off frequency 10 Hz) and several cardiac cycles were averaged to obtain an average pressure waveform.

Statistics

Group averaged pump function graphs were obtained by averaging Prv_{iso} and SVI_{max}.

Unpaired Student's *t*-test and Mann-Whitney *U* test were performed to compare data of both groups.

All data are presented in tables as mean ± SD in tables and in figures as mean ± SE or median values and interquartile ranges. A *P* value of < 0.05 was considered statistically significant.

Results

General Patient Characteristics

General patient characteristics are given in Table 1. Patients with SScPAH were significantly older with a mean age difference of 27 years. The SScPAH group consisted of 100% female patients, whereas in the IPAH group 77% of the patients were female. All the SScPAH patients included suffered from the limited cutaneous form of systemic sclerosis.

The 6-minute walk distance was not significantly different between the groups, as were values for mixed venous oxygen saturation and NT-proBNP. Evaluation of pulmonary function showed that pulmonary gas exchange in SScPAH patients, quantified by the transfer factor for carbon monoxide (TL_{CO}), was significantly lower compared to IPAH patients, in agreement with previously reported values(14, 15). Mean values of total lung capacity and evaluation by HRCT in the SScPAH group indicated that the pulmonary hypertension cannot be explained by severe pulmonary fibrosis: HRCT showed a typical pattern of pulmonary fibrosis in the dorsobasal lung fields in 7 of the 13 SScPAH patients; these patients had TLC levels of > 70% of predicted and SaO_2 levels of 92% and higher.

Haemodynamic invasive parameters and pump function graphs

Haemodynamic parameters are listed in Table 2. All patients had PVR values higher than 240 dynes·s·cm⁻⁵. A significantly lower mPap was found in the SScPAH group compared to the IPAH group. The mPrv was significantly lower in the SScPAH group than in the IPAH group, while SVI was not significantly different (Figure 3). There was no significant difference in total arterial load as neither PVR nor total arterial compliance was different between the groups (Figure 4).

To evaluate the cardiac pump function, we constructed pump function graphs as described above. Examples of individual pump function graphs of a SScPAH patient and a IPAH patient

are depicted in Figure 5. The averaged pump function graphs are shown in Figure 6. The $mPrv_{iso}$ was found to be significantly lower for SScPAH patients compared to IPAH patients. SVI_{max} did not differ between the two groups. Thus, compared to the SScPAH patients the IPAH patients demonstrated a higher pump function graph, 'rotated' around the same point of the horizontal axis intercept, i.e. SVI_{max} .

Discussion

In this study we compared the cardiac pump function between SS_cPAH patients and IPAH patients by using the relation between mean right ventricular pressure and stroke volume index. These variables were obtained by using standard right heart catheterisation and Fick cardiac output measurements. We found lower values for mPrv in the SS_cPAH group compared to the IPAH group, while stroke volume indices were not significantly different. Analysis of the arterial system in terms of PVR and total arterial compliance showed no difference in arterial load between the two groups. On the basis of these data we conclude that right heart pump function differs between the SS_cPAH and IPAH groups.

These haemodynamic differences between SS_cPAH and IPAH patients are in agreement with those described by Fisher *et al.*(4). Although they did not evaluate cardiac function, their haemodynamic data showed a similar pattern as ours consisting of a similar CI at lower mPap values. In their study, PVR was significantly lower SS_cPAH compared with IPAH in contrast to the comparable PVR values between the groups in our study cohort. This supports our data: despite lower afterload, SS_cPAH patients were not able to generate higher cardiac index compared to IPAH patients. In addition, they observed a significantly higher mortality in the SS_cPAH group compared to the IPAH group, despite the fact that IPAH patients had higher PVR, supporting the idea that cardiac involvement contributes to the early death in SS_cPAH. To characterize differences in cardiac function, we constructed a pump function graph per patient. A pump function graph presents the pumping ability of the right ventricle. Elzinga *et al.* have shown in isolated cat hearts that the pump function of the left and right heart can be described quantitatively by such a graph which relates mean ventricular pressure with mean ventricular output (16, 17). This relationship, which characterizes the heart, was determined by making the heart eject against a series of different arterial loads. Changing the afterload of an individual heart moves the pressure and flow values on this graph, i.e., increased load

decreases cardiac output and increases PRV. The pump function graph was shown to depend on heart rate, ventricular filling and cardiac muscle contractility i.e. muscle properties (6). By using stroke volume index instead of cardiac index, we avoided the effects of differences in heart rate. As schematically shown by Figure 1, an increase of end diastolic volume causes a parallel outward shift of the pump function graph, while increased contractility results in a rotation about the intercept on the SVI-axis. Thus, our data, by showing this rotation of the pump function graph to lower pressures but with a comparable intercept on the X-axis in SScPAH compared with IPAH, indicate lower contractility in the SScPAH group.

We used the single beat method to derive isovolumic right ventricular pressure from a measured ventricular pressure of an ejecting beat. Sunagawa *et al.* found that for the left ventricle there is a correlation between the isovolumic pressure (P_{iso}) observed during an isovolumic beat and the P_{iso} that is predicted by sine wave extrapolation from the isovolumic parts of an ejecting beat (12). Brimiouille *et al.* showed that this single-beat method can be used for the right ventricle as well (13). In this study, we used this method to predict the mean isovolumic pressure of the right ventricle ($mPrv_{iso}$) in individual patients to be able to describe a full pump function graph.

Since PVR and compliance did not differ we conclude that the difference in ventricular pressure between SScPAH and IPAH hearts is based on differences in performance of the heart itself.

The advantage of the use of the ventricular pump function graph is that it is based on standard catheterization measurements, Fick and PRV. However, this method still needs further validation in humans. Validation of the pump function graph method could be performed by the evaluation of difference of contractility between the SScPAH and IPAH groups by construction of a series of RV pressure-volume loops during the temporary occlusion of the inferior vena cava measured by means of a conductance catheter (18). However, this is an

intervention with substantial patient burden. Moreover, volume measurement with the conductance catheter in the RV is a possibility (19) but still not sufficiently evaluated. Another method would be to simultaneously measure RV pressure by right heart catheterisation and RV volume by MRI analysis; this method also needs further validation (20).

The lower contractility in SScPAH might be explained in several ways. Myocardial fibrosis as well as intramyocardial coronary vessel involvement are known to affect the ventricles in SSc (21, 22). Fernandes and co-workers (23) analyzed endomyocardial biopsies from SSc patients, with both limited and the diffuse cutaneous forms of SSc, without signs or symptoms of heart failure and excluded patients with pulmonary or arterial hypertension, left ventricular (LV) hypertrophy, and LV diastolic dysfunction. They demonstrated abnormal collagen deposition in 94% of the cases. Impaired contractility of hearts of patients with SScPAH might then be explained by increased extracellular matrix, which might affect normal contraction of the cardiac myocytes it surrounds (24, 25). Remodeling of the heart due to persistent elevations in ventricular developed pressure leads to changes in the amount of collagen, the collagen phenotype and collagen cross-linking (reviewed by Brower *et al.* (26)). Cross-linking has not been investigated in the hearts of SSc patients, but it is increased in skin with systemic sclerosis (27, 28). It may be speculated that SSc myocardial tissue expresses an increased degree in collagen cross-linking that contributes to an impaired cardiac contractility.

An impaired contractility in SScPAH could also be explained by ischemia due to vascular alterations. It has been shown that structural abnormalities of small coronary arteries or arterioles explains a reduced coronary reserve in SSc (29, 30).

Other underlying pathophysiological mechanisms may be found at the level of cardiac muscle per se. One of the mechanisms by which the cardiac muscle adapts to ventricular pressure overload is, under normal conditions, hypertrophying. However, impaired contractility of

SScPAH hearts might not be explained by an inability of the SScPAH heart to hypertrophy, as RV mass of SScPAH hearts has been shown to be comparable with RV mass of IPAH hearts (41.6 ± 12.3 (n=11) vs. 45.8 ± 14.8 g/m² (n = 14), $p = 0.51$) (31). This does not exclude that other intrinsic myocyte pathology may be responsible for impaired cardiac contractility in the SScPAH group, although information on this topic, for example on intrinsic myocyte abnormalities that may be responsible for impaired contractility in the SScPAH group, is not available. Our hypothesis of intrinsic myocardial involvement in SScPAH patients is supported by the findings of Meune et al (32), who found decreased RVEF in patients with early SSc (both LcSSc and DcSSc), without relation with mean pulmonary artery pressure. In our study group, the SScPAH patients were significantly older than the IPAH patients, reflecting the normal epidemiological features (15, 33). Age differences might affect RV diastolic function, but have not been demonstrated to affect RV systolic function (34, 35). To exclude, however, age-related factors as the underlying explanation of the found differences in our study, a study with age-matched SScPAH and IPAH patients may elucidate the influence of age on RV contractility in PAH. Other limitations are the weak power of this study due to the low patient numbers. Moreover, there is heterogeneity of patients as shown by the ranges of NT-proBNP values, PVR and Compliance.

The SScPAH population consisted of patients with the limited cutaneous form of SSc (8), which may lead to a bias since no DcSSc patients were studied. First, patients with the diffuse cutaneous form (DcSSc) are more likely to suffer from pulmonary fibrosis as a contributor or cause of pulmonary hypertension, and as our patient group consists of LcSSc patients with no or mild fibrosis on HRCT, we have not considered fibrosis as a potential cause of PH. We thus assume the SSc patients in the present study suffer from pulmonary hypertension caused by precapillary vasculopathy and in such a way are comparable with the IPAH patients. Second, it might be that cardiac involvement of SSc is different in DcSSc compared to LcSSc.

As differences in this respect have not been elucidated, it is difficult to extrapolate our findings to the diffuse cutaneous form of SSc (DcSSc), as no knowledge exists in respect of differences in heart involvement and adaptation in response of elevated PVR between LcSSc and DcSSc.

In conclusion, we have demonstrated, by using standard catheterization data, that SScPAH patients have lower cardiac contractility compared with IPAH patients. Further study of RV function in SScPAH should elucidate the underlying mechanisms.

Reference List

1. Hachulla E, Gressin V, Guillemin L, Carpentier P, Diot E, Sibilia J, Kahan A, Cabane J, Frances C, Launay D, Mouthon L, Allanore Y, Tiev KP, Clerson P, de Groote P, Humbert M. Early detection of pulmonary arterial hypertension in systemic sclerosis: a French nationwide prospective multicenter study. *Arthritis Rheum* 2005; 52: 3792-3800.
2. Mukerjee D, St George D, Coleiro B, Knight C, Denton CP, Davar J, Black CM, Coghlan JG. Prevalence and outcome in systemic sclerosis associated pulmonary arterial hypertension: application of a registry approach. *Ann Rheum Dis* 2003; 62:1088-1093.
3. Kawut SM, Taichman DB, Archer-Chicko CL, Palevsky HI, Kimmel SE. Hemodynamics and survival in patients with pulmonary arterial hypertension related to systemic sclerosis. *Chest* 2003; 123: 344-350.
4. Fisher MR, Mathai SC, Champion HC, Girgis RE, Houston-Harris T, Hummers L, Krishnan JA, Wigley F, Hassoun PM. Clinical differences between idiopathic and scleroderma-related pulmonary hypertension. *Arthritis Rheum* 2006; 54: 3043-3050.
5. Dorfmueller P, Humbert M, Perros F, Sanchez O, Simonneau G, Muller KM, Capron F. Fibrous remodeling of the pulmonary venous system in pulmonary arterial hypertension associated with connective tissue diseases. *Hum Pathol* 2007; 38: 893-902.
6. Westerhof N, Stergiopoulos N., Noble MIM. Pump function Graph. In: Westerhof N. Stergiopoulos N., Noble MIM. Snapshots of Hemodynamics; An aid for Clinical Research and Graduate Education. 1st Edn. Springer Science + Business Media, New York, 2005; pp.63-70.
7. Barst RJ, McGoon M, Torbicki A, Sitbon O, Krowka MJ, Olschewski H, Gaine S. Diagnosis and differential assessment of pulmonary arterial hypertension. *J Am Coll Cardiol* 2004; 43(12 Suppl S): 40S-47S.
8. LeRoy EC, Black C, Fleischmajer R, Jablonska S, Krieg T, Medsger TA, Jr., Rowell N, Wollheim F. Scleroderma (systemic sclerosis): classification, subsets and pathogenesis. *J Rheumatol* 1988; 15: 202-205.
9. Mahapatra S, Nishimura RA, Sorajja P, Cha S, McGoon MD. Relationship of pulmonary arterial capacitance and mortality in idiopathic pulmonary arterial hypertension. *J Am Coll Cardiol* 2006; 47: 799-803.
10. Chemla D, Hebert JL, Coirault C, Zamani K, Suard I, Colin P, Lecarpentier Y. Total arterial compliance estimated by stroke volume-to-aortic pulse pressure ratio in humans. *Am J Physiol* 1998; 27: H500-H505.
11. van den Horn GJ, Westerhof N, Elzinga G. Optimal power generation by the left ventricle. A study in the anesthetized open thorax cat. *Circ Res* 1985; 56:252-261.
12. Sunagawa K, Yamada A, Senda Y, Kikuchi Y, Nakamura M, Shibahara T, Nose Y. Estimation of the hydromotive source pressure from ejecting beats of the left ventricle. *IEEE Trans Biomed Eng* 1980; 27: 299-305.

13. Brimiouille S, Wauthy P, Ewalenko P, Rondelet B, Vermeulen F, Kerbaul F, Naeije R. Single-beat estimation of right ventricular end-systolic pressure-volume relationship. *Am J Physiol Heart Circ Physiol* 2003; 284: H1625-H1630.
14. Steen V, Medsger TA, Jr. Predictors of isolated pulmonary hypertension in patients with systemic sclerosis and limited cutaneous involvement. *Arthritis Rheum* 2003; 48: 516-522.
15. Stupi AM, Steen VD, Owens GR, Barnes EL, Rodnan GP, Medsger TA, Jr. Pulmonary hypertension in the CREST syndrome variant of systemic sclerosis. *Arthritis Rheum* 1986; 29: 515-524.
16. Elzinga G, Westerhof N. The effect of an increase in inotropic state and end-diastolic volume on the pumping ability of the feline left heart. *Circ Res* 1978; 42: 620-628.
17. Elzinga G, Westerhof N. How to quantify pump function of the heart. The value of variables derived from measurements on isolated muscle. *Circ Res* 1979; 44: 303-308.
18. Suga H, Sagawa K, Shoukas AA. Load independence of the instantaneous pressure-volume ratio of the canine left ventricle and effects of epinephrine and heart rate on the ratio. *Circ Res* 1973; 32: 314-322.
19. Baan J, van der Velde ET, de Bruin HG, Smeenk GJ, Koops J, van Dijk AD, Temmerman D, Senden J, Buis B. Continuous measurement of left ventricular volume in animals and humans by conductance catheter. *Circulation* 1984; 70: 812-823.
20. Kuehne T, Yilmaz S, Steendijk P, Moore P, Groenink M, Saaed M, Weber O, Higgins CB, Ewert P, Fleck E, Nagel E, Schulze-Neick I, Lange P. Magnetic resonance imaging analysis of right ventricular pressure-volume loops: in vivo validation and clinical application in patients with pulmonary hypertension. *Circulation* 2004; 110: 2010-2016.
21. Follansbee WP, Miller TR, Curtiss EI, Orie JE, Bernstein RL, Kiernan JM, Medsger TA, Jr. A controlled clinicopathologic study of myocardial fibrosis in systemic sclerosis (scleroderma). *J Rheumatol* 1990; 17: 656-662.
22. Owens GR, Follansbee WP. Cardiopulmonary manifestations of systemic sclerosis. *Chest* 1987; 91: 118-127.
23. Fernandes F, Ramires FJ, Arteaga E, Ianni BM, Bonfa ES, Mady C. Cardiac remodeling in patients with systemic sclerosis with no signs or symptoms of heart failure: an endomyocardial biopsy study. *J Card Fail* 2003; 9: 311-317.
24. Westerhof N, Boer C, Lamberts RR, Sipkema P. Cross-talk between cardiac muscle and coronary vasculature. *Physiol Rev* 2006; 86 : 1263-1308.
25. Lamberts RR, Willemsen MJ, Perez NG, Sipkema P, Westerhof N. Acute and specific collagen type I degradation increases diastolic and developed tension in perfused rat papillary muscle. *Am J Physiol Heart Circ Physiol* 2004; 286: H889-H894.
26. Brower GL, Gardner JD, Forman MF, Murray DB, Voloshenyuk T, Levick SP, Janicki JS. The relationship between myocardial extracellular matrix remodeling and ventricular function. *Eur J Cardiothorac Surg* 2006; 30: 604-610.

27. Chanoki M, Ishii M, Kobayashi H, Fushida H, Yashiro N, Hamada T, Ooshima A. Increased expression of lysyl oxidase in skin with scleroderma. *Br J Dermatol* 1995; 133: 710-715.
28. Brinckmann J, Neess CM, Gaber Y, Sobhi H, Notbohm H, Hunzelmann N, Fietzek PP, Muller PK, Risteli J, Gebker R, Scharffetter-Kochanek K. Different pattern of collagen cross-links in two sclerotic skin diseases: lipodermatosclerosis and circumscribed scleroderma. *J Invest Dermatol* 2001; 117: 269-273.
29. Bulkley BH, Ridolfi RL, Salyer WR, Hutchins GM. Myocardial lesions of progressive systemic sclerosis. A cause of cardiac dysfunction. *Circulation* 1976; 53: 483-490.
30. Kahan A, Nitenberg A, Foulst JM, Amor B, Menkes CJ, Devaux JY, Blanchet F, Perennec J, Lutfalla G, Roucayrol JC. Decreased coronary reserve in primary scleroderma myocardial disease. *Arthritis Rheum* 1985; 28: 637-646.
31. Overbeek MJ, Gan CT, Westerhof N, Voskuyl AE, Boonstra A, Postmus PE, Vonk Noordegraaf A. Cardiac contractility is impaired in systemic sclerosis-associated pulmonary hypertension compared to idiopathic pulmonary hypertension. *Am J Resp Crit Care Med* 2007; 175 (Abstract Issue): 1002.
32. Meune C, Allanore Y, Devaux JY, Dessault O, Duboc D, Weber S, Kahan A. High prevalence of right ventricular systolic dysfunction in early systemic sclerosis. *J Rheumatol* 2004; 31: 1941-1945.
33. Rich S, Dantzker DR, Ayres SM, Bergofsky EH, Brundage BH, Detre KM, Fishman AP, Goldring RM, Groves BM, Koerner SK, . Primary pulmonary hypertension. A national prospective study. *Ann Intern Med* 1987; 107: 216-223.
34. Fleg JL, O'Connor F, Gerstenblith G, Becker LC, Clulow J, Schulman SP, Lakatta EG. Impact of age on the cardiovascular response to dynamic upright exercise in healthy men and women. *J Appl Physiol* 1995; 78: 890-900.
35. Klein AL, Leung DY, Murray RD, Urban LH, Bailey KR, Tajik AJ. Effects of age and physiologic variables on right ventricular filling dynamics in normal subjects. *Am J Cardiol* 1999; 84: 440-448.

Table 1. General patient characteristics

	SScPAH	IPAH	P
	N=13	N=17	
Age, yrs	68.6 ± 12.4	41.9 ± 16.0	< 0.001
Female, no., (%)	13 (100)	13 (77)	< 0.001*
Limited cutaneous SSc, no. (%) [†]	13 (100)	-	-
Diffuse cutaneous SSc, no. (%) [†]	0 (0)	-	-
SSc disease duration, yrs [‡]	9.6 ± 6.8	-	-
	(n=12)		
Raynaud phenomenon duration, yrs	18 ± 15	-	-
Antibody profile: anti-centromere/anti-Scl-70/ anti-U1-RNP, no. (%)	7/1/1 (50/7/7)	-	-
Body surface area, m ²	1.7 ± 0.2	1.9 ± 0.3	0.005
Systolic ABP, mmHg	129 ± 22	119 ± 23	0.49
Diastolic ABP, mmHg	74 ± 13	73 ± 11	0.78
6-minute walk distance, m	277 ± 116	358 ± 110	0.08
SvO ₂ , %	62.0 ± 6.5	63.5 ± 6	0.68
NT-proBNP, pg/ml	3546 ± 3035	1384 ± 1160	0.24
	(n=10)	(n=9)	
TLC %	89.9 ± 16.6	99.9 ± 11.8	0.26
TL _{CO} %	42.8 ± 12.6	65.7 ± 16.1	0.002

Values expressed as mean ± SD or otherwise as stated. Abbreviations: SScPAH: systemic sclerosis-associated pulmonary arterial hypertension; IPAH: idiopathic pulmonary arterial

hypertension; anti-U1-RNP : anti-U1 ribonucleoprotein autoantibody ABP: arterial blood pressure; SvO₂: mixed venous oxygen saturation; NT-proBNP: non-terminal-pro brain natriuretic peptide; TLC %: percentage of predicted total lung capacity; TL_{CO} %: percentage of transfer factor for carbon monoxide. *Chi square statistic. † According to reference 13. ‡ Since first non-Raynaud symptom.

Table 2. Haemodynamics and pump function graph data

	SScPAH	IPAH	P
	N=13	N=17	
Heart rate, beats/min	82.4 ± 13.0	86.7 ± 13.8	0.43
Pra, mmHg	6 ± 4	8 ± 5	0.56
mPrv, mmHg	31 ± 9	41 ± 9	0.006
mPrv _{iso} , mmHg	43 ± 12	54 ± 10	0.043
sPrv, mmHg	43 ± 12	60 ± 10	< 0.0001
dPrv, mmHg	11 ± 5	14 ± 7	0.48
mPap, mmHg	44 ± 10	60 ± 10	< 0.0001
sPap, mmHg	70 ± 14	97 ± 19	< 0.0001
dPap, mmHg	26 ± 6	37 ± 8	< 0.0001
PCWP, mmHg	9 ± 34	8 ± 4	0.62
PVR, dynes·s·cm ⁻⁵	848 ± 397	1079 ± 433	0.13
Compliance, ml/mmHg	1.1 ± 0.42	0.9 ± 0.43	0.30
SVI, ml/m ²	27.1 ± 7.3	26.7 ± 7.6	0.84
SVI _{max} , ml/m ²	53.5 ± 20.6	57.5 ± 15.9	0.23
CI, l/min.m ²	2.2 ± 0.6	2.3 ± 0.6	0.71

Values expressed as mean ±SD. Definition of abbreviations: Pra, mPrv: mean right atrial and mean right ventricular pressures; mPrv_{iso}: mean of the RV maximal isovolumic beat; sPap, dPap mPap: systolic, diastolic and mean pulmonary artery pressures; PVR: pulmonary vascular resistance; Compliance: total pulmonary arterial compliance; SVI: stroke volume index; SVI_{max}: maximal SVI.

Figure Legends

Figure 1

A schematically drawn ventricular pump function graph, relating mean ventricular output (SVI) and mean ventricular pressure, and characterizing the heart as a pump. Alteration in contractility results in a rotation around the intercept on the output axis (SVI_{max}), while increased filling increases both $mPrv_{iso}$ and SVI_{max} . The three data points are the mean isovolumic RV pressure ($mPrv_{iso}$) at zero SVI, constructed using single beat method, the measured mean RV pressure and measured mean SVI (working point) and the (derived) maximum output SVI_{max} at zero pressure.

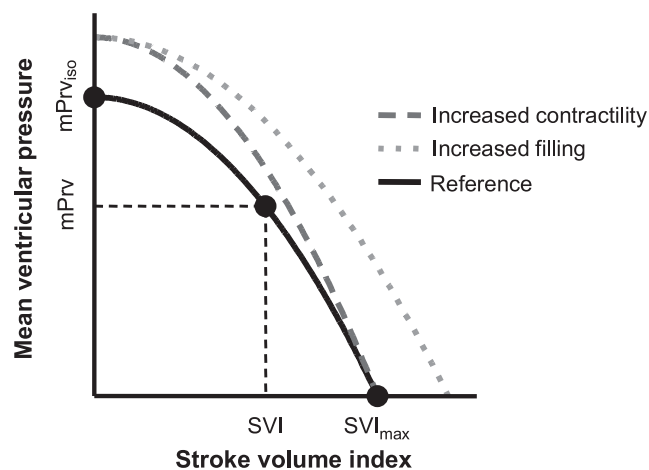


Figure 2

Schematic example of the derivation of an isovolumic beat. Isovolumic contraction is assumed to start at the minimum right ventricle pressure (Prv), before the steep rise of the pressure (indicated by point 1), and to end when it reaches diastolic pulmonary artery pressure (Pap , indicated by point 2). The isovolumic relaxation period is defined from the pulmonary artery valve closure (point 3), identified from deviation of Prv and Pap , till the ventricular

pressure reaches the diastolic pressure level (point 4). The area under the Prv curve is used to calculate mPrv; the total area under the short dashed line (Prv_{iso}) is used to calculate the mean isovolumic RV pressure (mPrv_{iso}).

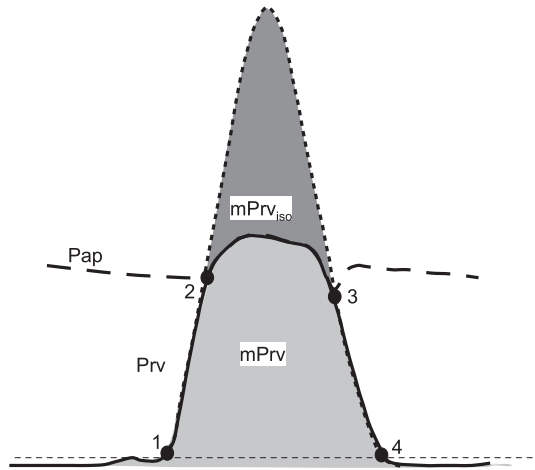


Figure 3

Mean right ventricular pressure (mPrv), left, and stroke volume index (SVI), right, in systemic sclerosis-associated pulmonary arterial hypertension (SScPAH) and idiopathic pulmonary arterial hypertension (IPAH). Data are presented as a boxplot, where the black horizontal bar is the median, the box is the interquartile range and the vertical lines extend to the smallest and largest observations.

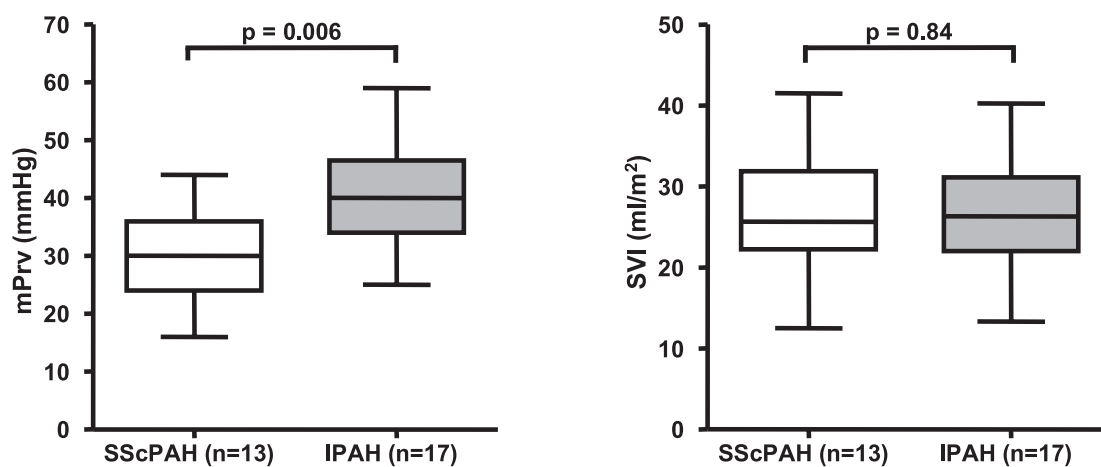


Figure 4

The arterial load: Pulmonary vascular resistance (PVR), left, and pulmonary arterial compliance, right, in systemic sclerosis-associated pulmonary arterial hypertension (SScPAH), and idiopathic pulmonary arterial hypertension (IPAH). Data are presented as a boxplot, where the black horizontal bar is the median, the box is the interquartile range and the vertical lines extend to the smallest and largest observations.

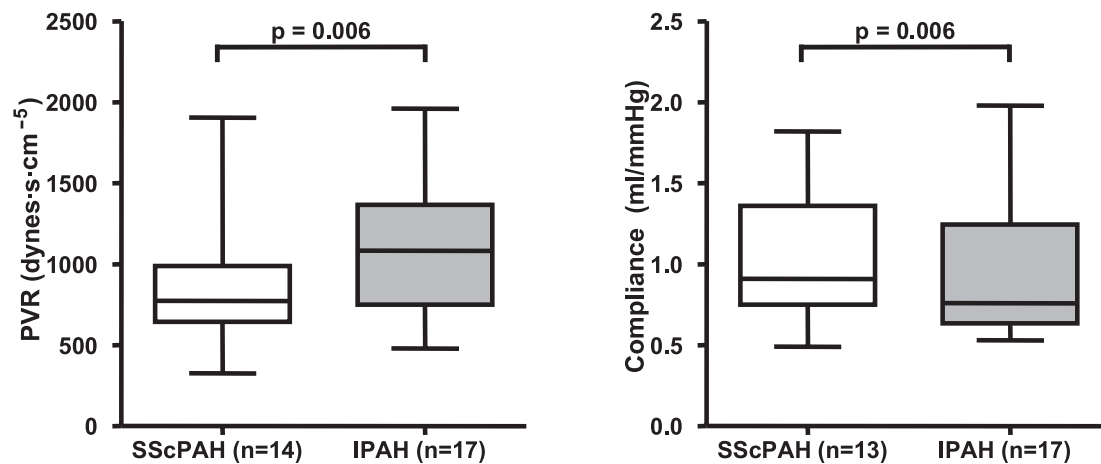


Figure 5

Examples of pump function graphs of two patients. A patient with systemic sclerosis-associated pulmonary arterial hypertension (SScPAH), left, and idiopathic pulmonary arterial hypertension (IPAH), right.

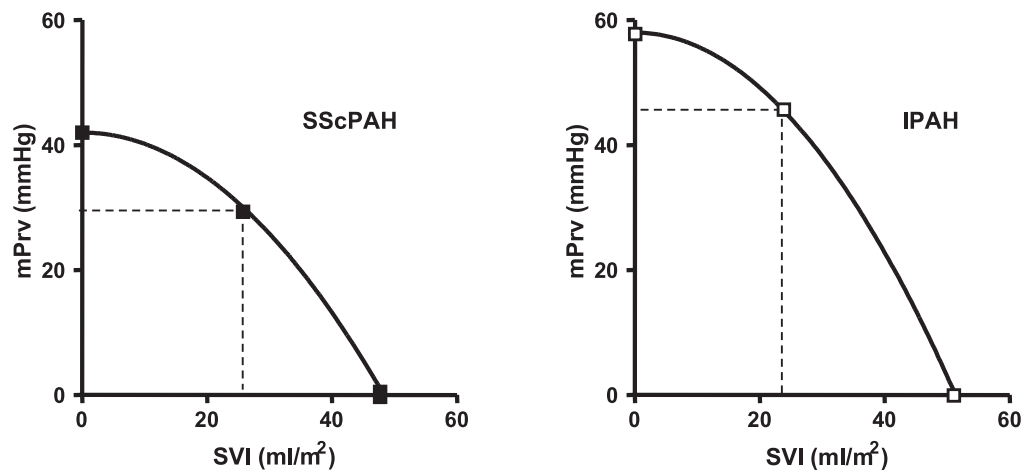


Figure 6.

The averaged ventricular pump function graph for systemic sclerosis-associated pulmonary arterial hypertension (SScPAH) and idiopathic pulmonary arterial hypertension (IPAH).

Individual SScPAH patients are represented by the filled squares, individual IPAH patients by the non-filled squares. The three data points with SE bars are plotted for each group: mean isovolumic right ventricular pressure ($mPrv_{iso}$), with stroke volume (SVI) zero, measured $mPrv$ against measured SVI and the maximal SVI, SVI_{max} , at zero $mPrv$. The IPAH pump function graph is located above the SScPAH pump function graph, with a rotation around the SVI_{max} .

